On nonlinear wave-structure interaction using an immersed boundary method in 2D. *

Stavros Kontos[a], Harry B. Bingham[a], Ole Lindberg[a] and Allan P. Engsig-Karup[b]

[a] Mechanical Engineering and [b] Applied Mathematics & Computer Science
Technical University of Denmark

Email: stakon@mek.dtu.dk, hbb@mek.dtu.dk, old@force.dk, apek@dtu.dk

1 Introduction

We present our progress on the development and preliminary benchmarking results of a new efficient methodology for solving fully non-linear potential flow wave-structure interaction problems. The new model utilises the efficiency of finite difference methods on structured grids. The structure geometry is introduced using an Immersed Boundary Method (IBM) and the body boundary condition (BC) is satisfied with a Weighted Least Squares (WLS) approximation [7]. This allows complex geometries to be represented with high accuracy. The stability of the scheme is ensured by adopting the Weighted Essentially Non-Oscillatory (WENO) scheme [8] together with a Lax-Friedrichs type flux applied to the free surface conditions in Hamilton-Jacobi form. This work can be viewed as a novel extension of the flexible order finite difference potential flow solver OceanWave3D [2] to include the presence of a structure. The method obtains an optimum scaling of the solution effort [2] and has been implemented on massively parallel GPU architectures using the CUDA API [3] making it suitable for high resolution flow simulations. This combination of novel and robust numerical methods aims at creating new efficient tools for non-linear wave-structure interaction problems. The scheme is validated using the forced heaving motion of a two-dimensional (2D) horizontal circular cylinder with promising results, although there are still challenges to be overcome in terms of properly capturing the behavior of the intersection between the body and the free-surface.

2 Mathematical formulation

A Cartesian coordinate system $(\mathbf{x}, z) = (x, y, z)$ is adopted with the z-axis vertical and x-axis in the direction of the body's forward motion. The potential flow initial-boundary-value problem is presented below:

$$\nabla^2\phi + \partial_{zz}\phi = 0, \quad \text{in } \mathcal{V} \tag{2.1a}$$

$$\partial_t\zeta + \nabla\zeta\left(\nabla\tilde{\phi} - \tilde{w}\,\nabla\zeta - \mathbf{U}\right) = \tilde{w}, \quad \text{on } z = \zeta \tag{2.1b}$$

$$\partial_t\tilde{\phi} + \nabla\tilde{\phi}\left(\frac{1}{2}\nabla\tilde{\phi} - \mathbf{U}\right) - \frac{1}{2}\tilde{w}^2\left(1 + \nabla\zeta\nabla\zeta\right) = -g\zeta, \quad \text{on } z = \zeta \tag{2.1c}$$

$$\partial_z\phi + \nabla h\nabla\phi = 0, \quad \text{on } z = -h \tag{2.1d}$$

$$\partial_n\phi = V_n \quad \text{on } \mathcal{S}_b \tag{2.1e}$$

where $\zeta(\mathbf{x}, t)$ is the free surface (FS) elevation, $\phi(\mathbf{x}, z, t)$ is the velocity potential, $h(\mathbf{x})$ is the sea bottom, $\nabla = (\partial_x, \partial_y)$ is the horizontal gradient operator and $\mathbf{U} = (U, 0)$ is the body forward velocity vector. $\mathcal{S}_b(t)$ stands for the moving body surface, $V_n(\mathbf{x}, z, t)$ represents the normal component of velocity of a point on the ship surface and ∂_n is the derivative in the direction normal to $\mathcal{S}_b$. The overbar denotes quantities evaluated on the free surface. For a freely-floating body a coupling with Newton's law is required. However, in the current abstract only 2D forced motion problems are considered.

*The authors wish to thank the EU 7th Framework Programme (Grant Agreement number 605221, SHOPERA) and the Danish Innovation Fund grant no. 4106-00038B for funding.

3 Numerical solution

The boundary value problem (2.1) is solved numerically by mapping the solution with a sigma transformation to a time-invariant computational domain as discussed in [2]. To keep this transformation smooth and continuous, the free surface is extended into the interior of the body by creating an artificial interior free surface as shown in Figure 4.1. In that way, the wetted body surface is also mapped to the computational domain. The computational domain is a unit-spaced Cartesian mesh. The classical explicit fourth-order, four-stage Runge-Kutta scheme is used for time-stepping. In each Runge-Kutta stage the following algorithm is executed:

- Compute the position and the velocity of the body.
- Construct the new interior free-surface.
  - Calculate the elevation of the outermost interior FS points by extrapolating the exterior FS values. If the point lies in the exterior of the body a new exterior FS point is added and the search continues until the first interior FS point is found. A Courant number $C_r < 1$ ensures that maximum one FS point can be added per time-step.
  - Find the body-free surface intersection. Tracking the intersection robustly is challenging and the method is still under development. At the moment the Bisection Iteration method between the first interior and exterior FS points is used.
  - Connect the two intersection points with the interior FS. Two continuous x-derivatives over the entire FS are required for the sigma transform. Fulfilling this requirement with a well behaved curve is a challenge that is still in progress. Currently a 9-th order polynomial is fitted between the intersection points. The six boundary conditions are the extrapolated ζ, ζ_x, ζ_{xx} on each point. The extra degrees of freedom are used to keep the polynomial well behaved by minimizing it's square distance from the straight line between the two points.
- If a new exterior FS point is added, its ζ and $\tilde{\phi}$ values are computed by extrapolation.
- Solve the Laplace problem by using the IBM-WLS methods for satisfying the body boundary condition.
- Step forward in time the free-surface boundary conditions using WENO for the spatial discretization (automatic upwinding).

4 Weighted Least Squares, Immersed Boundary Method body boundary condition

The coupling of the WLS, IBM body boundary condition approximation with the finite difference approximation of the Laplace equation is described in detail in [7]. A sign function is used to distinguish the interior and exterior to the body points. The interior points that belong to a fluid point stencil are identified as ghost points. The Laplace equation is only solved on fluid points. A normal projection from the ghost points to the body surface is used to identify the body points where the body BC is satisfied. The ghost points adjacent to the body-FS intersection are used to satisfy the body BC on these locations. A WLS stencil is formed for each body point, using fluid points in a centred stencil around it plus the associated ghost point. The WLS method is then used to approximate the normal derivative of the body BC.

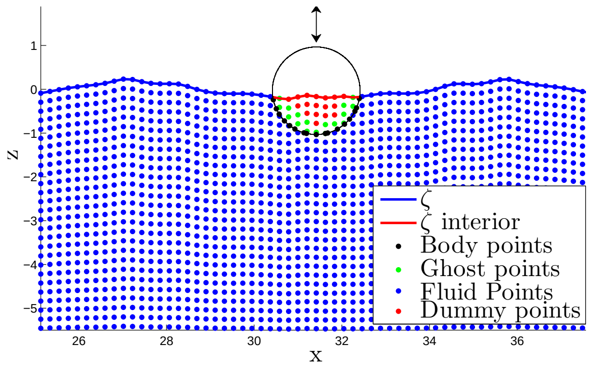

Figure 4.1: Non-linearly oscillating cylinder with a large amplitude motion $A/R = 0.2$

5 Hamilton-Jacobi WENO formulation of the Free Surface Boundary Conditions

To apply WENO on the free surface boundary conditions, they have to be expressed in Hamilton-Jacobi form: $\boldsymbol{\phi}_t + H(\nabla\boldsymbol{\phi}) = 0$. For the spatial discretization the Lax-Friedrichs scheme is used [8]:

$$\hat{H} = H\left(\frac{\phi_x^- + \phi_x^+}{2}, \frac{\phi_y^- + \phi_y^+}{2}\right) - a^x\left(\frac{\phi_x^+ - \phi_x^-}{2}\right) - a^y\left(\frac{\phi_y^+ - \phi_y^-}{2}\right) \tag{5.1}$$

where ϕ_x^-, ϕ_x^+ are the left- and right-biased WENO derivative approximations. The a^x and a^y are dissipation coefficients for controlling the amount of numerical viscosity. They are defined as $a^x = \max|H_1(\phi_x, \phi_y)|$, and $a^y = \max|H_2(\phi_x, \phi_y)|$. H_1 and H_2 are the partial derivatives of H with respect to ϕ_x and ϕ_y, respectively. The 2D FS boundary conditions can be expressed in the WENO formulation as:

$$\partial_t\zeta + H_\zeta = \partial_z\tilde{\phi}; \qquad H_\zeta = \partial_x\zeta\left(\partial_x\tilde{\phi} - \partial_z\tilde{\phi}\,\partial_x\zeta - U\right) \tag{5.2}$$

$$\partial_t\tilde{\phi} + H_\phi = -g\zeta; \qquad H_\phi = \partial_x\tilde{\phi}\left(\frac{1}{2}\partial_x\tilde{\phi} - U\right) - \frac{1}{2}(\partial_z\tilde{\phi})^2\,(1 + \partial_x\zeta\,\partial_x\zeta) \tag{5.3}$$

The right hand side terms are considered as source terms. More details and testing of the formulation can be found in [6].

6 Test cases

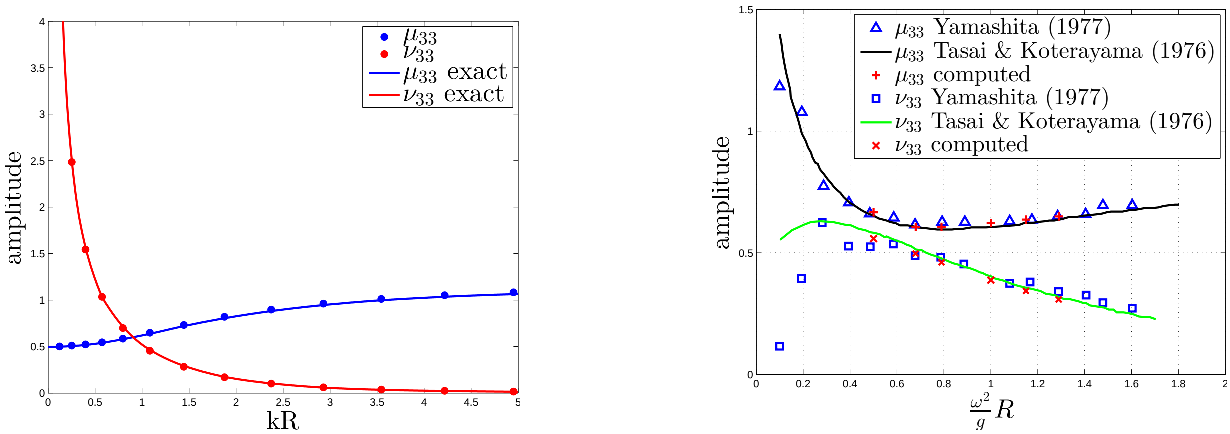

(a) Linearized case.

(b) Non-linear large amplitude case.

Figure 6.1: Comparison of the computed hydrodynamic coefficients with the literature.

The linearized radiation problem of a heaving half-submerged cylinder is considered first. The body displacement follows a Gaussian profile as in [11] and introduces a Gaussian range of frequencies. The comparison with the analytical results of [1] is good as shown in Figure 6.1a. In anticipation of solving free-motion problems, we avoid using the Bernoulli equation directly, and compute the force on the cylinder using a form derived for example in [9]:

$$F = -\rho \frac{d}{dt} \iint_{\mathcal{S}_b} \phi \mathbf{n} \, dS + \rho \iint_{\mathcal{S}_b} (\partial\phi/\partial n \nabla\phi - \frac{1}{2}\nabla\phi \cdot \nabla\phi \mathbf{n}) \, dS \tag{6.1}$$

where in the linear case the second term is omitted. As a second test, the fully non-linear forced heaving motion of a cylinder with radius R is studied. The prescribed motion of its center of mass is $z_{g3}(t) = z_{g3}(0) + A\sin(\omega t)$. The angular frequency is selected such that $\omega^2 R/g = 1$. The sea bottom is at $h = \lambda$. For comparison with the results of [5] the cylinder radius is set to $R = 1\ m$, the gravitational acceleration to $g = 1\ m/s^2$ and the density to $\rho = 1\ kg/m^3$. As a first step a small amplitude motion is considered where $A = 0.01R$. The added-mass and damping results for two discretizations $N_f = \lambda/dx$ are compared with reference values from the literature in the following table:

	μ_{33}	ν_{33}
$N_f = 40$	0.601	0.390
$N_f = 60$	0.603	0.396
Porter (1960)	0.58	0.41
Frank (1967)	0.62	0.40
Kent (2005)	0.582	0.410

The same calculations were done for a large amplitude motion $A = 0.2R$ and the results are presented in Figure 6.1b. The comparison is relatively good, but we note that the force signal contained periodic jump discontinuities which were filtered out to obtain these results. We speculate that these jumps in the solution are connected with an inconsistency in either the IBM method or the treatment of the free-surface/body intersection point, or both. Solving this issue is our current challenge.

References

[1] Bai, K. J., 1977. *The added mass of two-dimensional cylinders heaving in water of finite depth.* Journal of Fluid Mechanics, 81(1), pp. 85105.

[2] Engsig-Karup, A. P., Bingham, H. B., Lindberg, O., 2009. *An efficient flexible-order model for 3d nonlinear water waves.* Journal of Computational Physics, 228:2100-2118.

[3] Engsig-Karup, A. P., Madsen, M. G., Glimberg, S. L., 2012. *A massively parallel GPU-accelerated model for analysis of fully nonlinear free surface waves.* International Journal for Numerical Methods in Fluids, 70(1):20-36, 2012.

[4] Frank, W., 1967. *Oscillation of cylinders in or below the free surface of deep fluids.* DTIC Document, Report 2375. Naval Ship Research and Development Center, Hydromechanics Laboratory, Washington, D.C., USA.

[5] Kent, C., 2005. *A pseudo-spectral method for calculating wave-body interaction using an explicit free-surface formulation.* PhD thesis, University of Michigan.

[6] Kontos, S., Bingham, H. B., Lindberg, O., Engsig-Karup, A. P., 2015. *A robust WENO scheme for nonlinear waves in a moving reference frame.* Journal of Hydrodynamics, submitted.

[7] Lindberg, O., Bingham, H. B., Engsig-Karup, A. P., 2014. *Towards Real Time Simulation of Ship-Ship Interaction-Part III: Immersed Body Boundary Condition and Double Body Ship-Ship Interaction.* IWWWFB 29.

[8] Liu X. D., Osher S., Chan T., 1994. *Weighted ENO Schemes for Hamilton-Jacobi Equations.* Journal of Computational Physics, Vol. 115, Issue 1, November 1994, pp. 200212.

[9] Newman, J. N., 1977. *Marine Hydrodynamics.* MIT Press, 1 Jan 1977.

[10] Porter, W., 1960. *Pressure distributions, added-mass, and damping coefficients for cylinders oscillating in a free surface.* Technical report, DTIC Document.

[11] Read, R. W., Bingham. H. B., 2012. *An overset grid approach to linear wave-structure interaction.* ASME 2012 31st International Conference on Ocean, Offshore and Arctic Engineering Volume 4.

[12] Tasai, F., Koterayama, W., 1976. *Nonlinear hydrodynamic forces acting on cylinders heaving on the surface of a fluid.* Rep. Res. Inst. Appl. Mech. Kyushu Univ. 24:1-39

[13] Yamashita, S., 1977. *Calculations of the hydrodynamic forces acting upon thin cylinders oscillating vertically with large amplitude.*J. Soc. Nav. Arch. 141:61-70.